Uncorrected Proof

Water Science & Technology

Water Science & Technology Vol 00 No 0, 1 doi: 10.2166/wst.2022.379

Proficient exclusion of pesticide using humic acid-modified magnetite nanoparticles from aqueous solution

Arti Jangra [a], Jai Kumar [a], Devender Singh [b], Harish Kumar [c], Parvin Kumar [a], Suresh Kumar [a] and Ramesh Kumar [a,*]

[a] Department of Chemistry, Kurukshetra University, Kurukshetra 136119, India
[b] Department of Chemistry, Maharshi Dayanand University, Rohtak 124001, India
[c] Department of chemistry, School of Basic Sciences, Central University of Haryana, Mahendergarh 123029, India
*Corresponding author. E-mail: rameshkumarkuk@gmail.com; rameshchemkuk@kuk.ac.in

AJ, 0000-0003-4113-3451; JK, 0000-0003-2556-6345; DS, 0000-0002-2180-5049; HK, 0000-0002-8559-2302; PK, 0000-0002-2635-6465; SK, 0000-0003-0602-767X; RK, 0000-0003-2089-2213

ABSTRACT

Extensive dispersal of the pesticides to shield the different types of vegetation from pests has increased the production but at the same it has resulted into increase in environmental pollution. Consequently, it is necessary to eliminate these undesired pollutants from the environment. The current investigation offers the synthesis of humic acid-coated magnetite nanoparticles towards effective removal of the most common insecticide, imidacloprid from the aqueous solution using batch adsorption method. These synthesized nanoparticles were characterized with the help of several analytical and spectroscopic techniques. To acquire the maximum conceivable adsorption, effects of different influencing parameters like pH of the solution, time of contact, concentration of pesticide solution, amount of adsorbent and temperature were also examined. Moreover, the kinetic studies were found to be in good agreement with pseudo-second-order kinetic model supporting the occurrence of chemisorption phenomenon. Additionally, isotherm modeling proved that the adsorption process was in accordance with Langmuir model of isotherm. Thermodynamic parameters depicted the endothermic and spontaneous behavior of the adsorption process. Desorption studies were also carried out to examine the reusability of these nano-adsorbent. These verdicts confirmed that the surface modified magnetite nanoparticles may be treated as proficient material for exclusion of imidacloprid from the aqueous solution.

Key words: adsorption, co-precipitation, magnetite nanoparticles, pesticide, surface modification

HIGHLIGHTS

- Humic acid functionalized magnetite nanoparticles were employed as proficient tool for the removal of pesticide from the aqueous solution.
- Kinetic studies established the occurrence of chemisorption phenomenon.
- Monolayer adsorption was confirmed with the help of isotherm modeling.
- Thermodynamic studies confirmed the adsorption process to be endothermic and spontaneous in nature.

GRAPHICAL ABSTRACT

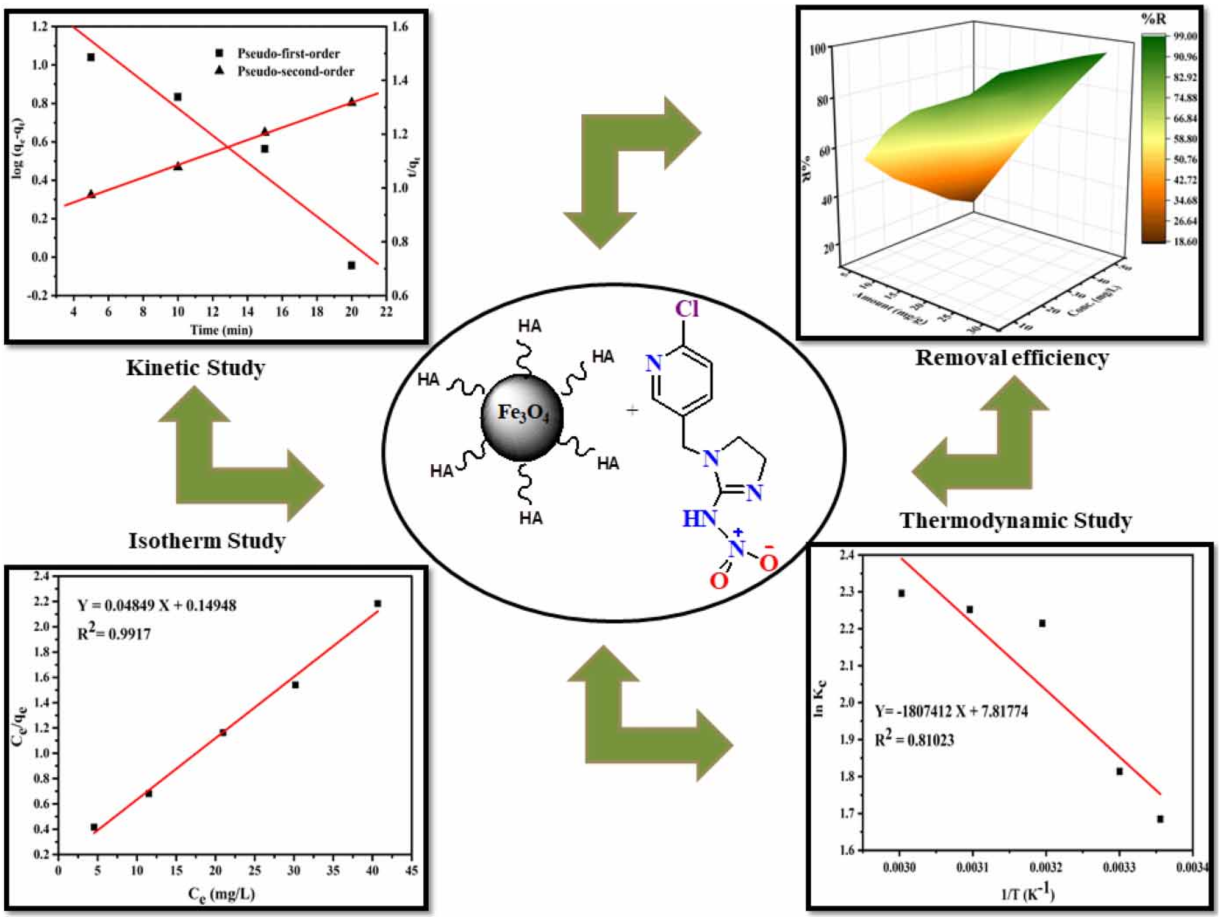

1. INTRODUCTION

During the past few decades, use of agrochemicals has been increased vastly for improving the crop production to fulfil the food necessities of the world's escalating population (Rahbar *et al.* 2022). However, the increased and imbalanced usage of the pesticides contaminate the environment severely which further poses serious threats to the food quality, human wellbeing, soil quality and ecological balance (Rani *et al.* 2021). Imidacloprid (IMCP) is a common insecticide and is being vastly used for eliminating various kinds of insects that have harmful impact on the crops. The remnants of the pesticides tend to remain in the biological system; therefore, the risk towards human and aquatic lives has been increased significantly. Thus, the need of the hour is to explore the cost-effective and ecofriendly methods to eliminate the pesticide remnants. During the past few years, several methods have been reported for the removal of pesticide remnants (Sun *et al.* 2019; Zhao *et al.* 2019; Ghernaout & Elboughdiri 2020; Pohl 2020; Shah & Shah 2020; Liang *et al.* 2021; Ma *et al.* 2021; Rathi & Kumar 2021; Ghosh *et al.* 2022). Among these, adsorption method has received significant attention of the scientists working in this field because of its low cost and better results. In adsorption method, various kind of adsorbents have been reported for the removal of imidacloprid remnants from the aqueous solution. For instance, work has been reported on the use of agri waste bio-char, normal bio-char and phosphoric acid treated bio-char for the removal of imidacloprid from the aqueous solution (Mandal & Singh 2017; Mandal *et al.* 2017). Heat treated kerolite have also been reported as adsorbent for the adsorption of imidacloprid pesticide from the aqueous solution (Socías-Viciana *et al.* 2003). Similarly, investigation on adsorption of imidacloprid using activated carbon obtained from oilseed has been reported (Yao Urbain *et al.* 2018). Prompted by these studies, in the present work, we wish to report the humic acid modified magnetite nanoparticles as proficient nano-adsorbent for the removal of imidacloprid pesticide from the aqueous solution. Moreover, we have also compared the results of our study with already reported close work for the removal of imidacloprid from the aqueous solution. It is pertinent to mention that percentage removal of imidacloprid using humic acid modified magnetite nanoparticles was found much higher as compared to already reported conventional adsorbents.

The current work also elucidated the effects of several parameters like pH of the solution, contact time, quantity of adsorbent and initial concentration of imidacloprid on the percentage removal efficiency of humic acid modified magnetite nanoparticles as nano-adsorbent for the removal of imidacloprid from the aqueous solution. In addition to this, the isotherm, kinetic and thermodynamic studies were also performed. The results of the isotherm studies suggested that the adsorption process followed Langmuir isotherm model of isotherm which is based on the assumption that there are defined number of active sites with no competition between them and the adsorption occur in a location independent of the occupied adjacent active sites. Further, the adsorption process was found to obey pseudo-second-order kinetics which suggested it to be chemisorption. Moreover, the reported nano-adsorbents can be separated easily from aqueous solution using external magnetic field and can also be reused for the adsorption of imidacloprid contaminants. Therefore, the humic acid modified magnetite nanoparticles may be considered as effective and proficient adsorbent for the adsorption of imidacloprid pesticide from aqueous solution.

2. MATERIALS AND METHODS

2.1. Materials

Ferric chloride hexahydrate ($FeCl_3 \cdot 6H_2O$), Ammonium hydroxide (25%), Ferrous sulfate heptahydrate ($Fe_2SO_4 \cdot 7H_2O$) and humic acid (HA) were bought from SRL (India) while Imidacloprid was obtained from Sigma Aldrich. All solutions were prepared using distilled water throughout the experiments.

2.2. Methods and analytical techniques

A digital mechanical stirrer set (2,000 rpm) was used to prepare magnetic nanoparticles by co-precipitation method. A fourier transform infrared spectrometer (FTIR), (model MB-3000ABB) was used to record the IR spectra. Thermograms were obtained using a thermogravimetric analyzer, Perkin Elmer STA-6000 with 5–80 °C/min heating rate and in 20–1,000 °C temperature range. Hitachi SU-8000 field emission scanning microscope (FESEM) was used to determine the size and surface morphology of nanoparticles. Additionally, the average size of the nanoparticles was measured by particle size analyzer (Microtrac W3602). X-ray diffraction (XRD) patterns were recorded on X-ray diffractometer retaining Cu Kα radiation having 1.540 A° wavelength. The absorbance of solutions at variable concentrations was determined using a UV-visible spectrophotometer (T90 PG) in the range of 900–190 nm.

2.3. Preparation of magnetite nanoparticles and surface functionalization

The bare magnetite nanoparticles (MNPs) were synthesized by adopting a simple and cost effective co-precipitation method. After that their surface was modified with humic acid as reported in our previous work (Jangra *et al.* 2021). In brief, 6.1 g of $FeCl_3 \cdot 6H_2O$ and 4.2 g of $FeSO_4 \cdot 7H_2O$ were dissolved in 100 mL distilled water. This mixture was agitated vigorously using digital mechanical stirrer at a speed of 2,000 rpm under nitrogen atmosphere. The temperature was maintained between 85 and 90 °C during this process. After 20 minutes, 25% ammonium hydroxide was added rapidly to the stirring mixture (pH ~9–10). Appearance of black colored suspension confirmed the formation of magnetite nanoparticles (Fe_3O_4). In order to obtain the humic acid coated magnetite nanoparticles (HA@Fe_3O_4), a solution of humic acid was added to the above formed black colored suspension. The mixture was stirred further for about 30 min under the same reaction condition. Thus formed humic acid coated magnetite nanoparticles (HA@Fe_3O_4) were separated from the solution using external magnetic field. These isolated surface modified nanoparticles were cautiously washed with distilled water to exclude spare amount of ammonia and dehydrated using vacuum oven.

2.4. IMCP adsorption tests on surface functionalized magnetite nanoparticles

The synthesized humic acid coated magnetite nanoparticles were employed as adsorbent for the removal of selected pesticide i.e. imidacloprid from the aqueous solution. The batch technique was used throughout the experiments. Effect on adsorption of imidacloprid on the surface of functionalized magnetite nanoparticles was examined by varying different parameters like contact time, pH of solution, amount of adsorbent, temperature and initial concentration of pesticide. After the separation of adsorbent from the solution by using external magnetic field, the concentration of IMCP in the aqueous solution was measured by UV-visible spectrophotometer by recording absorbance at maximum wavelength, 270 nm. The percentage removal efficiency and adsorption capacity at equilibrium was obtained using Equations (1) and (2), respectively:

$$\text{Percentage removal efficiency, } \%R = \frac{C_0 - C_e}{C_0} \times 100 \tag{1}$$

$$\text{Adsorption capacity, } q_e = \frac{C_0 - C_e}{m} \times V \tag{2}$$

where, C_0 and C_e (mg/L) are the initial and equilibrium concentrations, respectively. q_e(mg/g), m (g) and V (L) are the equilibrium adsorption capacity, adsorbent amount and volume of the solution used, respectively.

2.5. Desorption study

A desorption experiment was performed to evaluate the reusability of $HA@Fe_3O_4$ nanoparticles. 30 mg of humic acid coated magnetite nanoparticles with imidacloprid adsorbed on their surface ($IMCP@HA@Fe_3O_4$ nanoparticles) were mixed with 10 mL of desorbing solvent and stirred for about 100–120 min at room temperature. Then, the $HA@Fe_3O_4$ nanoparticles were separated from the solution using a magnet and the absorbance of the decanted solution was measured at 270 nm. The desorption capacity (q_{de}) was calculated using Equation (3):

$$\text{Desorption capacity, } q_{de} = \frac{C_{de}V}{m} \tag{3}$$

where C_{de} (mg/L) is the pesticide concentration in desorbing solvent, V is the volume of desorbing solvent used, and m is the mass of $IMCP@HA@Fe_3O_4$ nanoparticles.

Whereas, the percentage of desorption efficiency (W_{de}) can be calculated by using Equation (4):

$$\text{Percentage desorption efficiency, } \%W_{de} = \frac{q_e}{q_{de}} \times 100 \tag{4}$$

After desorption, the humic acid coated nanoparticles were separated out and dried. After that, the adsorption capacity of recycled nanoparticles was investigated again to examine the reusability of these nanoparticles.

3. RESULTS AND DISCUSSION

3.1. Characterization of nanoparticles

3.1.1. Fourier transform infrared spectral analysis of surface functionalized MNPs

The IR spectrum of bare magnetite nanoparticles was compared with that of surface functionalized magnetite nanoparticles. The strong peak near 600 cm^{-1} may be associated to Fe-O stretching vibration while the absorption bands around 3,300 cm^{-1} may be attributed to –O-H stretching vibration of magnetite nanoparticles. However, in the IR spectrum of surface functionalized magnetite nanoparticles new peaks at 1,638 and 1,416 cm^{-1} were observed that may be assigned to asymmetric and symmetric stretching respectively, of carboxylate anion of the coating material, (Jangra *et al.* 2021). The IR spectrum of humic acid functionalized magnetite nanoparticles showed all the peaks that were present in the individual IR spectrum of the bare magnetite nanoparticles and pure humic acid. These findings confirmed the successful coating of humic acid on the surface of bare magnetite nanoparticles.

3.1.2. Field emission electron microscope analysis

From the field emission electron microscope (FESEM) images it was observed that the diameter of bare magnetite nanoparticles and humic acid coated magnetite nanoparticles was around 20 and 30 nm, respectively (Jangra *et al.* 2021). The increase in diameter of nanoparticles also suggested the effective coating of humic acid over the surface of magnetite nanoparticles.

3.1.3. X-ray diffraction analysis

X-ray diffraction (XRD) patterns of the bare magnetite nanoparticles and humic acid coated magnetite nanoparticles were recorded over the 2θ range of 20°–80°. The XRD pattern of both Fe_3O_4 and $HA@Fe_3O_4$ nanoparticles showed six characteristic peaks which clearly indicated about their semi-crystalline nature (Jangra *et al.* 2021).

3.1.4. Thermogravimetric analysis

Thermogram of both bare and coated magnetite nanoparticles showed weight loss upto 100 °C that may be accredited to the moisture loss. As expected, no further changes were perceived in the case of Fe_3O_4 nanoparticles while $HA@Fe_3O_4$ nanoparticles exhibited a significant weight loss over the temperature range of 200–500 °C due to thermal decay of coating material i.e. humic acid (Jangra *et al.* 2021).

3.2. IMCP adsorption studies by modified magnetite nanoparticles

Various preliminary experimental studies were accomplished to estimate the influences of several factors such as pH of solution, time, adsorbent dose and initial concentrations of pollutant solution on the adsorption of imidacloprid over the surface of $HA@Fe_3O_4$.

3.2.1. Impact of pH on the percentage removal efficiency of $HA@Fe_3O_4$ nanoparticles

The pH of the solution plays a vital role in the adsorption process because it may affect the surface charge of the adsorbate and adsorbent. From the 3D surface graphs, it was clear that the percentage uptake efficiency of $HA@Fe_3O_4$ nanoparticles for the imidacloprid increased gradually with an increase in the pH of solution from 2 to 7 (Figure 1) and later a decrease in percentage uptake efficiency was observed with increase in concentration of adsorbate solution in the range of 10–50 mg/L. These observations suggested that the highest percentage of IMCP uptake was attained at pH 7 for 10 mg/L owing to the neutral state of IMCP at pH 7. Therefore, it can be concluded that the nano-adsorbent showed remarkable adsorption at neutral condition. The decrease in adsorption at low pH could be explained on account of protonation of functional groups of pesticide, IMCP as well as coating material of magnetite nanoparticles i.e. humic acid. Electrostatic repulsion between positively-charged species lowers the adsorption of IMCP on the adsorbent in acidic condition. On the contrary, hydrogen bonding and electrostatic interactions between adsorbate and adsorbent was observed maximum at pH 7. At higher pH, the decrease in the percentage removal of imidacloprid may be justified on the basis of electrostatic repulsion between the negatively charged surfaces of the adsorbate and adsorbent. Therefore, it may be concluded that maximum adsorption of imidacloprid on the surface of nano-adsorbent can be achieved at pH 7.

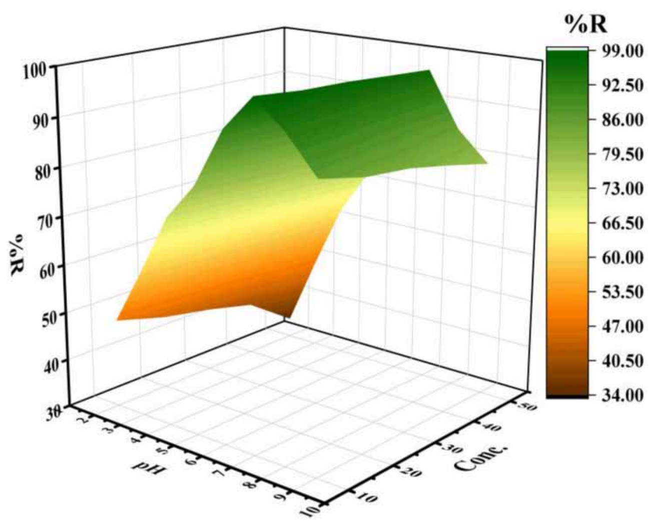

Figure 1 | Effect of pH on percentage removal at variable concentration of adsorbate.

3.2.2. Time effect and kinetic modeling

The equilibrium and kinetic studies play a significant role in the adsorption technique and help in the examination of the adsorption capacity of adsorbent with passage of time. Kinetic models provide information regarding the adsorption kinetic and probable mechanism involved therein. The pseudo-first-order model is based on the assumption that the rate of change of solute uptake with time is directly proportional to difference in saturation concentration and the amount of solid uptake with time, which is generally termed as physical sorption. While, the pseudo-second-order kinetic model indicate the adsorption process to be chemisorption. The kinetic and equilibrium studies were carried out for variable amount of adsorbent i.e. HA@Fe_3O_4 (05–30 mg) in 10 mL of imidacloprid solution (50 mg/L) at specific pH. Figure 2 suggested the improvement in percentage removal efficiency of nano-adsorbent upto 30 minutes after which a stage of equilibrium was attained and no further change was observed in the percentage removal efficiency. These outcomes suggested that all activated sites of this nano-adsorbent were completely occupied in 30 minutes after which no adsorption took place. At the equilibrium stage, 30 mg of nano-adsorbent showed the highest percentage removal of imidacloprid.

Furthermore, based upon these investigations, various kinetic models such as pseudo-first-order and pseudo-second-order kinetic models were studied, simultaneously (Figure 3). Lagergren-first-order (Hagos Kahsay *et al.* 2020) and pseudo-second-order (Ho & McKay 1999; Amar *et al.* 2022) kinetic equations (Equations (5) and (6), respectively) were used to study the rate of adsorption process:

$$\log(q_e - q_t) = \log q_e - \frac{k_1 t}{2.303} \tag{5}$$

$$\frac{t}{q_t} = \frac{1}{k_2 q_e^2} + \frac{t}{q_e} \tag{6}$$

where, q_e and q_t denotes the adsorption capacity in mg/g at equilibrium point and at any time, t, respectively. k_1 and k_2 are the rate constants for pseudo-first and pseudo-second-order kinetics. These calculated parameters have been summarized in Table 1. The comparison of the correlation coefficients obtained from the linear graph of these equations confirmed that the adsorption process fit better with the pseudo-second-order kinetic model inferring the occurrence of chemisorption process.

3.2.3. Impact of amount of adsorbent and initial concentration of pesticide solution

The influence of amount of nano-adsorbent on the percentage removal of imidacloprid from the aqueous solution was examined using 10 mL of imidacloprid solution of variable concentrations (10–50 mg/L) containing different amount of nano-

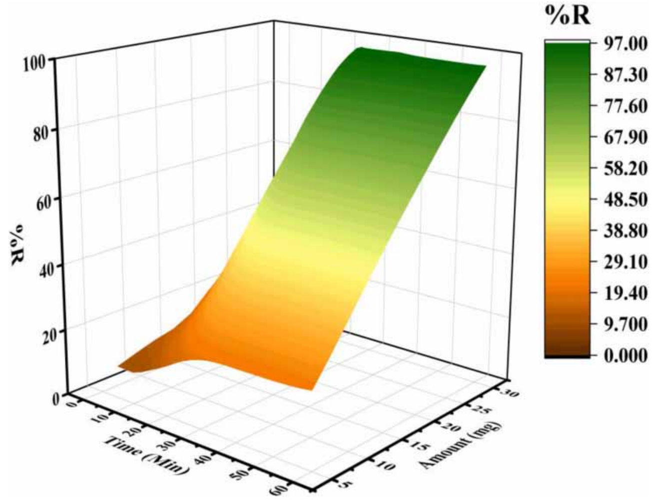

Figure 2 | Effect of contact time on percentage removal of imidacloprid for different amount of nano-adsorbent.

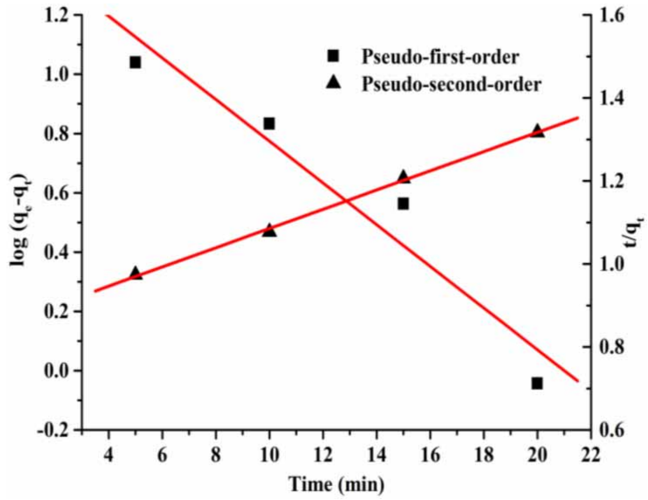

Figure 3 | Pseudo-first-order and Pseudo-second-order kinetic models.

Table 1 | Parameters of kinetic models

Pseudo-first-order			Pseudo-second-order		
R^2	k_1 (min^{-1})	q_e (mg/g)	R^2	k_2 (g mg^{-1} min^{-1})	q_e (mg/g)
0.9342	0.1619	4.38	0.9983	31.471	1.171

Where q_e is the adsorption capacity at equilibrium, k_1, k_2 and R are the rate constants and correlation coefficients for respective kinetic order.

adsorbent (5–30 mg) at fixed pH and temperature. The results obtained from the different experiments suggested that the percentage removal efficiency of the nano-adsorbent increased by increasing the amount of nano-adsorbent and decreased with an increase in initial concentration of IMCP solution, (Figure 4). It was observed that a maximum of 96.47% and a minimum of 18.64% of IMCP were removed from the aqueous solution of IMCP (concentration 50 mg/L) for 30 and 5 mg amount of nano-adsorbent (HA@Fe_3O_4), respectively. This can be justified on the account of the fact that greater the amount of

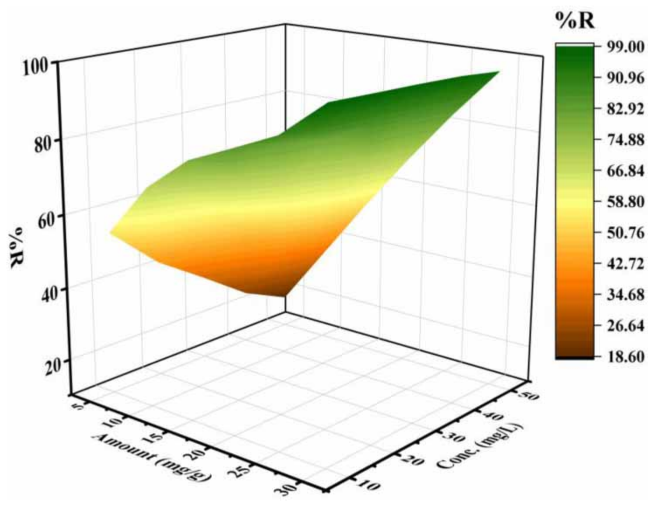

Figure 4 | Effect of amount of adsorbent on percentage removal at different concentration of pesticide solution.

adsorbent greater will be the availability of binding sites on the surface of adsorbent for the adsorption of adsorbate. However, at lowest pesticide concentration (10 mg/L), a maximum of 98.89% and a minimum of 54.57% of IMCP were removed for 30 and 5 mg of the adsorbent (HA@Fe_3O_4), respectively. This indicated that percentage removal of imidacloprid from the aqueous solution is higher at low concentration of pesticide solution (10 mg/L) than at maximum concentration of pesticide solution (50 mg/L).

3.2.4. Isotherm modeling

Under the optimal conditions, several isotherms models including Langmuir (Saxena *et al.* 2020), Freundlich (Kalhor *et al.* 2018) and Temkin (Annavi & Manickam 2022) were employed to study the nature of interactions between adsorbate and adsorbent in the adsorption process. Langmuir model of isotherm defines the removal capability of adsorbent on a homogenous surface which further suggests a single layer adsorption whereas Freundlich isothermic model depicts about heterogeneous or multilayer adsorption process. Temkin model implies a linear reduction in the adsorption heat of all adsorbent molecules due to the covering from adsorbate and adsorbent interactions. Linear forms of equations (Table 2) were used to evaluate the applicability of these models. The graphs were plotted by using these equations which helped in the calculation of different experimental parameters including maximum adsorption capacity, Langmuir, Freundlich and Tempkin isotherm constants as well as correlation coefficients (Table 3). The correlation coefficient (R^2) of Langmuir isotherm was found to be 0.9917, while for Freundlich and Tempkin isotherm it was found to be 0.8009 and 0.8291, respectively. Thus, from the R^2 values, it may be concluded that the process of adsorption of imidacloprid on the surface of HA@Fe_3O_4 nanoparticles was found to fit better with Langmuir isotherm model indicating that the adsorption process strongly followed the Langmuir model of isotherm (Figure 5).

3.2.5. Effect of variation in temperature and calculation of thermodynamic parameters

To study the effect of variation in temperature on the percentage removal of imidacloprid from the aqueous solution, a number of experiments were executed at variable temperatures using a fixed amount of adsorbent (30 mg) and 10 mL of IMCP solution (50 mg/L) at fixed value of pH i.e. 7. The outcomes of these experiments revealed that the percentage removal efficiency of nano-adsorbent gradually increased upto 313 K and after that a decrease in percentage removal efficiency was observed (Figure 6). To summarize, 313 K might be considered as the optimum temperature for the maximum adsorption at fixed value of pH and contact time.

Table 2 | Linear forms of isothermic equations

Isotherm	Linear Equations
Langmuir	$\frac{C_e}{q_e} = \frac{1}{bq_m} + \frac{C_e}{q_m}$
Freundlich	$\log q_e = \log K_F + \frac{1}{n}\log C_e$
Temkin	$q_e = B\ln A + B\ln C_e, \quad B = \frac{RT}{b}$

Where, q_m and q_e, represents the maximum adsorption capacity and adsorption capacity at equilibrium, b is the Langmuir constant, n and K_f are Freundlich constants while A and B denotes the Temkin constants.

Table 3 | Experimental parameters of isotherm models

Langmuir			Freundlich			Temkin		
R^2	q_m (mg/g)	B (L/mg)	R^2	N	K_F (mg/g)	R^2	A (L/mg)	B (J/mol)
0.9917	20.63	0.32	0.8009	3.984	2.48	0.8291	5.62	3.69

Where R denotes the correlation coefficients for respective isotherm models.

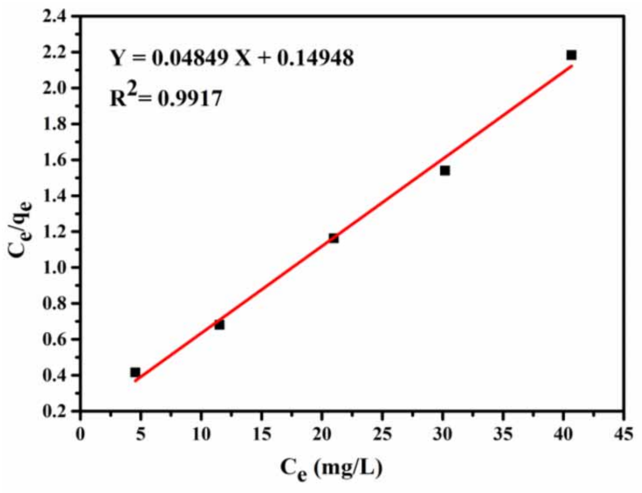

Figure 5 | Langmuir isotherm model.

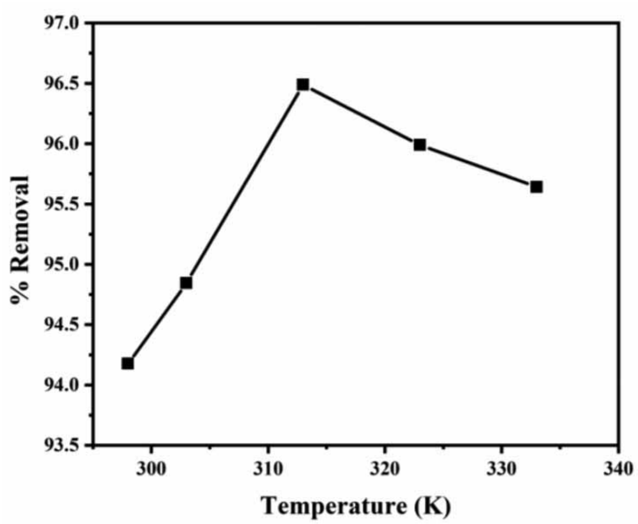

Figure 6 | Effect of temperature on percentage removal.

Related thermodynamic parameters such as change in gibbs free energy (ΔG), enthalpy (ΔH) and entropy change (ΔS), can be computed using Equations (5)–(7):

$$\Delta G = \Delta H - T\Delta S \tag{5}$$

$$\Delta G = -RT\ln K_c, \quad K_c = \frac{q_e}{C_e} \tag{6}$$

$$\textit{Hence}, \ \ln K_c = \frac{\Delta S}{R} - \frac{\Delta H}{RT} \tag{7}$$

The values of ΔS and ΔH can be obtained from intercept and slope of linear graph plotted between log K_c versus 1/T. Remarkably, the negative values of ΔG at all temperature specify the spontaneous and favorable nature while positive values of ΔH and ΔS depicted the endothermic nature of adsorption process (Ngo *et al.* 2022) as well as the high degree of freedom between adsorbent and adsorbate molecules (Figure 7).

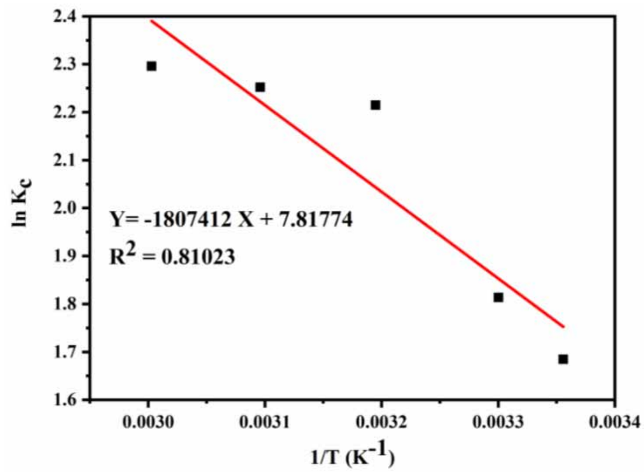

Figure 7 | Graph between ln K_c and 1/T for the calculation of thermodynamic parameters.

3.3. Comparison of percentage removal of imidacloprid by HA@Fe_3O_4 nanoparticles with other reported adsorbents

The percentage removal of imidacloprid by humic acid functionalized magnetite nanoparticles was compared with already reported adsorbents (Table 5). The comparative study revealed that humic acid functionalized magnetite nanoparticles are the most potential candidate among them for the removal of imidacloprid residues from the aqueous solution.

3.4. Proposed adsorption mechanism of adsorption of imidacloprid on the surface of HA@Fe_3O_4 nanoparticles

The adsorption of imidacloprid pesticide from aqueous solution by humic acid modified magnetite nanoparticles may be explained well on the basis of different functional groups present on the surface of these nano-adsorbents. Imidacloprid may be adsorbed onto the surface of humic acid modified magnetite nanoparticles via different kind of interactions like H-bonding, π-π interactions and electrostatic interactions (Keshvardoostchokami *et al.* 2018). The adsorption of imidacloprid on the surface of humic acid modified magnetite nanoparticles was found maximum at pH 7.0 as at this pH, hydrogen bonding and electrostatic attractions between them is maximum.

3.5. Desorption analyses

Desorption study was performed to evaluate the adsorbent regeneration and recovery of adsorbate. The desorption study revealed that a maximum of 80% pesticide was desorbed from the surface of humic acid modified magnetite nanoparticles after a period of 100–120 min. Additionally, no significant change was observed in the adsorption capacity of recycled HA@Fe_3O_4 nanoparticles which suggested that these nanoparticles can be reused again for the adsorption of pesticide from an aqueous solution.

Table 4 | Calculated thermodynamic parameters

Temperature (K)	ln K_c	ΔG (kJ/mol)	ΔH (kJ/mol K)	ΔS (J/ mol K)
298	1.68456	−4.174	15.026	64.996
303	1.81346	−4.568		
313	2.21462	−5.763		
323	2.25185	−6.047		
333	2.29613	−6.357		

Where ΔG, ΔH and ΔS represent gibbs free energy, enthalpy and entropy change, respectively.

Table 5 | Comparison of percentage removal efficiency of several adsorbents reported in literature

Sr. No.	Adsorbent used	pH	Isotherm	Kinetic order	% Removal of Imidacloprid	References
1.	Normal and Phosphoric acid treated Rice Straw bio-char	7	Freundlich	Pseudo-second-order	95	Mandal & Singh (2017)
2.	Agri waste bio-char	7	Freundlich	Pseudo-second-order	89.5	Mandal *et al.* (2017)
3.	Heat treated Kerolite	7	Freundlich	-	87.2	Socías-Viciana *et al.* (2003)
4.	Activated carbon from oilseed sell	6.9	Langmuir	Pseudo-first-order	90	Yao Urbain *et al.* (2018)
5.	Silver@graphene nano-composite	6.6	Freundlich	Pseudo-second-order	63	Keshvardoostchokami *et al.* (2018)
6.	Chitosan functionalized silver nanoparticles	6	–	Pseudo-second-order	85	Moustafa *et al.* (2021)
7.	Chitosan	6	–	Pseudo-second-order	40	Moustafa *et al.* (2021)
8.	Nano-porous activated carbon	5.2	Langmuir	Pseudo-second-order	80	Mohammad & El-Sayed (2021)
9.	HA@Fe_3O_4 nanoparticles	7	Langmuir	Pseudo-second order	96.47	The Present Study

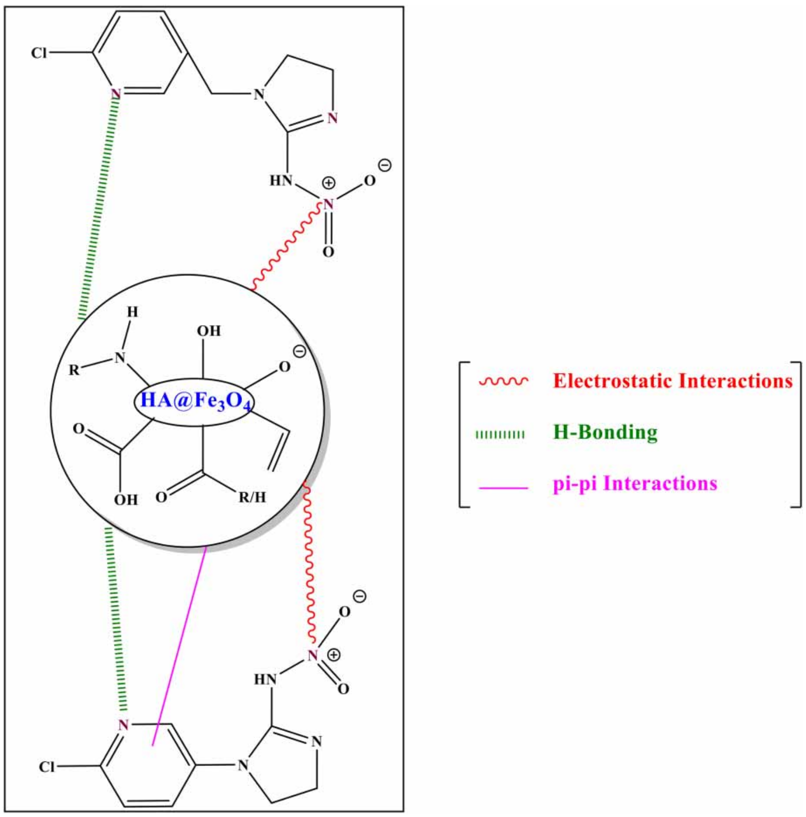

Figure 8 | Proposed mechanism for the adsorption of imidacloprid on the surface of humic acid functionalized magnetite nanoparticles (HA@Fe_3O_4).

4. CONCLUSION

In the continuation of our previously reported work, in which humic acid coated magnetite nanoparticles were prepared for the removal of crystal violet dye from the aqueous solution, the present work describes the use of these surface functionalized magnetite nanoparticles for the removal of imidacloprid pesticide from the aqueous solution. Effect of various factors including pH, contact time, amount of adsorbent, initial concentration of pesticide solution and temperature on the removal of imidacloprid from the aqueous solution was also examined. The results obtained from these studies suggested that the adsorption process attained the point of equilibrium after 30 min at pH 7 with 96.47% removal of imidacloprid for 30 mg of the adsorbent i.e. HA@Fe_3O_4. The adsorption process was found to follow pseudo-second-order-kinetic model suggesting the process to be chemisorption in nature. Further, the adsorption process was found to be best fitted with Langmuir model of isotherm. Thermodynamic analysis illustrated the endothermic and spontaneous nature of adsorption of IMCP on the surface of humic acid modified magnetite nanoparticles. Desorption study confirmed the reusability of these nano-adsorbents for the removal of imidacloprid from the aqueous solution. Thus, the overall study led to the conclusion that the humic acid coated magnetite nanoparticles can be used as proficient tool for the removal of imidacloprid from the aqueous solution.

ACKNOWLEDGEMENTS

The author and co-authors appreciatively acknowledges the UGC (University Grant Commission) for providing financial support in the form of SRF (senior research fellowship); Award no. 115576 and 134490.

DATA AVAILABILITY STATEMENT

All relevant data are included in the paper or its Supplementary Information.

CONFLICT OF INTEREST

The authors declare there is no conflict.

REFERENCES

Amar, I. A., Zayid, E. A., Dhikeel, S. A. & Najem, M. Y. 2022 Biosorption removal of methylene blue dye from aqueous solutions using phosphoric acid-treated balanites aegyptiaca seed husks powder. *Biointerface Research in Applied Chemistry* **12** (6), 7845–7862.

Annavi, A. & Manickam, M. 2022 Fabrication of iron nanoparticles from tea waste as an efficient adsorbent towards the removal of profenofos pesticide from aquatic environment. *International Journal of Environmental Analytical Chemistry*, 1–20.

Ghernaout, D. & Elboughdiri, N. 2020 Electrochemical technology for wastewater treatment: dares and trends. *Open Access Library Journal* **07** (01), 1–17.

Ghosh, N., Das, S., Biswas, G. & Haldar, P. K. 2022 Review on some metal oxide nanoparticles as effective adsorbent in wastewater treatment. *Water Science and Technology* **85** (12), 3370–3395.

Hagos Kahsay, M., Belachew, N., Tadesse, A. & Basavaiah, K. 2020 Magnetite nanoparticle decorated reduced graphene oxide for adsorptive removal of crystal violet and antifungal activities. *RSC Advances* **10** (57), 34916–34927.

Ho, Y. S. & McKay, G. 1999 Pseudo-second order model for sorption processes. *Process Biochemistry* **34** (5), 451–465.

Jangra, A., Singh, J., Khanna, R., Kumar, P., Kumar, S. & Kumar, R. 2021 Comparative studies of dye removal efficiency of surface functionalized nanoparticles with other adsorbents: isotherm and kinetic study. *Asian Journal of Chemistry* **33** (12), 3031–3038.

Kalhor, M. M., Rafati, A. A., Rafati, L. & Rafati, A. A. 2018 Synthesis, characterization and adsorption studies of amino functionalized silica nano hollow sphere as an efficient adsorbent for removal of imidacloprid pesticide. *Journal of Molecular Liquids* **266** (2017), 453–459.

Keshvardoostchokami, M., Bigverdi, P., Zamani, A., Parizanganeh, A. & Piri, F. 2018 Silver@ graphene oxide nanocomposite: synthesize and application in removal of imidacloprid from contaminated waters. *Environmental Science and Pollution Research* **25** (7), 6751–6761.

Liang, C., Wei, D., Zhang, S., Ren, Q., Shi, J. & Liu, L. 2021 Removal of antibiotic resistance genes from swine wastewater by membrane filtration treatment. *Ecotoxicology and Environmental Safety* **210**, 111885.

Ma, G., Xu, X., Tesfai, M., Zhang, Y., Wang, H. & Xu, P. 2021 Nanocomposite cation-exchange membranes for wastewater electrodialysis: organic fouling, desalination performance, and toxicity testing. *Separation and Purification Technology* **275**, 119217.

Mandal, A. & Singh, N. 2017 Optimization of atrazine and imidacloprid removal from water using biochars: designing single or multi-staged batch adsorption systems. *International Journal of Hygiene and Environmental Health* **220** (3), 637–645.

Mandal, A., Singh, N. & Purakayastha, T. J. 2017 Characterization of pesticide sorption behaviour of slow pyrolysis biochars as low cost adsorbent for atrazine and imidacloprid removal. *Science of the Total Environment* **577**, 376–385.

Mohammad, S. G. & El-Sayed, M. M. H. 2021 Removal of imidacloprid pesticide using nanoporous activated carbons produced via pyrolysis of peach stone agricultural wastes. *Chemical Engineering Communications* **208** (8), 1069–1080.

Moustafa, M., Abu-Saied, M. A., Taha, T., Elnouby, M., El-shafeey, M., Alshehri, A. G., Alamri, S., Shati, A., Alrumman, S., Alghamdii, H. & Al-Khatani, M. 2021 Chitosan functionalized AgNPs for efficient removal of imidacloprid pesticide through a pressure-free design. *International Journal of Biological Macromolecules* **168**, 116–123. https://doi.org/10.1016/j.ijbiomac.2020.12.055.

Ngo, V. D., Hoang, L. T. A., Pham, V. C., Ngo, V. H. & Tran, P. H. 2022 Estimation of pesticide residues on leafy vegetables using a developed handheld spectrometer. *Biointerface Research in Applied Chemistry* **12** (6), 8163–8173.

Pohl, A. 2020 Removal of heavy metal ions from water and wastewaters by sulfur-containing precipitation agents. *Water, Air, and Soil Pollution* **231** (10), 1–17.

Rahbar, N., Parsaie, A. & Baezat, M. R. 2022 Evaluation of imidacloprid adsorption on a new activated carbon based nanocomposite consisting of magnetite and copper oxide nanoparticles: adsorption modelling, optimisation, and characterisation. *International Journal of Environmental Analytical Chemistry*, 1–19.

Rani, L., Thapa, K., Kanojia, N., Sharma, N., Singh, S., Grewal, A. S., Srivastav, A. L. & Kaushal, J. 2021 An extensive review on the consequences of chemical pesticides on human health and environment. *Journal of Cleaner Production* **283**, 124657.

Rathi, B. S. & Kumar, P. S. 2021 Application of adsorption process for effective removal of emerging contaminants from water and wastewater. *Environmental Pollution* **280**, 116995.

Saxena, M., Sharma, N. & Saxena, R. 2020 Highly efficient and rapid removal of a toxic dye: adsorption kinetics, isotherm, and mechanism studies on functionalized multiwalled carbon nanotubes. *Surfaces and Interfaces* **21**, 100639.

Shah, A. & Shah, M. 2020 Characterisation and bioremediation of wastewater: a review exploring bioremediation as a sustainable technique for pharmaceutical wastewater. *Groundwater for Sustainable Development* **11**, 100383.

Socías-Viciana, M., González-Pradas, E., Saifi, M., Ureña-Amate, M. D., Flores-Céspedes, F. & Fernández-Pérez, M. 2003 The potential removal of imidacloprid from water by heat-treated kerolites. *Pest Management Science* **59** (10), 1162–1168.

Sun, Y., Zhou, S., Chiang, P.-C. & Shah, K. J. 2019 Evaluation and optimization of enhanced coagulation process: water and energy nexus. *Water-Energy Nexus* **2** (1), 25–36.

Yao Urbain, K., Kouadio Fodjo, E., Ardjouma, D., Yapi Serge, B., Serge Aimé, E., Bi Irié Marc, G. & Albert, T. 2018 Removal of imidacloprid using activated carbon produced from ricinodendron heudelotii shells. *Bulletin of the Chemical Society of Ethiopia* **31** (3), 397–409.

Zhao, Z., An, H., Lin, J., Feng, M., Murugadoss, V., Ding, T., Liu, H., Shao, Q., Mai, X., Wang, N., Gu, H., Angaiah, S. & Guo, Z. 2019 Progress on the photocatalytic reduction removal of chromium contamination. *The Chemical Record* **19** (5), 873–882.

First received 21 September 2022; accepted in revised form 11 November 2022. Available online 17 November 2022